

Supporting Information

Reconfigurable Three-Dimensional Gold Nanorod Plasmonic Nanostructures on DNA Origami Tripod

Content:

- I. Materials and methods
- II. Theoretical calculations
- III. Supporting figures
- IV. DNA sequences
- V. References

I. Materials and methods

Synthesis of gold nanorods. A two-step method was used to synthesize gold nanorod according to reference.¹

a. Synthesis of seeds: A 50 μ L of 2% (w/v) HAuCl₄ solution and 9.5 mL of 100 mM CTAB solution were added to a 20 mL flask. A 600 μ L of ice-cold NaBH₄ solution (10 mM) was added to the flask under vigorous stirring for 2 minutes. The color of the reaction solution changed to yellowish brown quickly. The resulting solution will stay 2 hours for the next step. The resulting solution will act as nucleation points of gold nanorods in the next step.

b. Synthesis of AuNR: In a 20 mL flask, 10 mL of 100 mM CTAB (hexadecyl-trimethyl-ammonium bromide) was first added, followed by the addition of 78 μ L of 2% (w/v) HAuCl₄ solution. A 80 μ L of 10 mM AgNO₃ was then added into the mixture sequentially to produce light yellowish color. Then 48 μ L of 0.1 M ascorbic acid was injected into the solution with moderate 5s shaking. Upon the addition of ascorbic acid, the yellowish solution gradually became colorless. Finally, 16 μ L of seed was injected and the flask was stirring for 1-2 minutes. The colorless solution turned to red, purple, and brown. The resultant mixture was left undisturbed at 30°C for 12 h for NR growth. The final products were isolated by centrifugation at 8,000 rpm for 10 min followed by removal of the supernatant. No size or shape-selective fractionation was performed. The pellet was suspended in 100 μ L water. The concentration was measured by UV spectra (UV2550, Shimadzu) using extinction coefficient of $1 \times 10^9 \text{ M}^{-1}\text{cm}^{-1}$ for the longitudinal plasmon resonance of the AuNRs.

Functionalization of AuNRs with DNA. Functionalization of AuNRs with thiolated DNA

(5'-TTTTTTTTTTTTAGCG-SH-3' for handle-1;

5'-TATAATAATAATATT-TT-SH-3' for handle-2;

5'-TTATAACTATTCCCTAAAAA-SH-3' for handle-3)

was carried out following the low pH route.² Four milliliter of 1 nM AuNRs was mixed with 40 μ L of 1% sodium dodecyl sulfate (SDS), 400 μ L of 10× TBE, and 100 μ L of 100 μ M DNA. Hydrochloric acid (HCl) was used to adjust the pH value of the solution to 3. The disulfide bond in the thiolated oligonucleotides was reduced to monothiol using Tris(carboxyethyl) phosphine hydrochloride (TCEP) (20 mM, 1 hr) in water. The oligonucleotides were purified using size exclusion columns (G-25, GE Healthcare) to get rid of the small molecules. The purified DNA was added to AuNR solution (OD~1) containing 0.01% (w/v) SDS with a molecular ratio of 4000: 1. After incubation of the AuNRs with DNA for 1 hour, 5 M NaCl was added to bring the final concentration of NaCl to 500 mM. The solution was then gently shaken overnight. After that, AuNR-DNA conjugates were centrifuged at 8000 rpm for 25 minutes. The pellet was suspended in 1 mL 0.5×TBE buffer containing 200 mM NaCl while the supernatant was discarded. The same centrifugation was repeated three times

to remove the excessive thiolated DNA completely. The final concentration of AuNRs was estimated with UV-Vis absorption spectroscopy using extinction coefficient of $1 \times 10^9 \text{ M}^{-1}\text{cm}^{-1}$ for the longitudinal plasmon resonance of the AuNRs.

Agarose gel electrophoresis. Annealed DNA origami samples and AuNR decorated tripod structures were subjected to agarose gel electrophoresis for purification. Samples were run in 1% agarose gel in a $0.5 \times \text{TBE-Mg}^{2+}$ buffer (45 mM Tris, 45 mM Boric acid, 1 mM EDTA, 10 mM MgCl_2) at 60V for 3 h within an ice-water bath.

II. Theoretical calculations

We present a theoretical study of the optical response of the symmetric triple nanorods (TNRs) based on mode-coupling analysis and the finite-difference time-domain (FDTD) simulation. To gain the basic mechanism, we first perform a mode-coupling analysis. Each nanorod (NR) is modeled by an oscillator (with oscillation amplitude a , b , or c). The coupling among the oscillators is described by the following equations

$$\ddot{a} + \omega_0^2 a + \gamma \dot{a} + tb + tc = E_a,$$

$$\ddot{b} + \omega_0^2 b + \gamma \dot{b} + tc + ta = E_b,$$

$$\ddot{c} + \omega_0^2 c + \gamma \dot{c} + tb + ta = E_c,$$

Where oscillation frequency ω_0 is the plasmon resonance frequency (depending on the aspect ratio of the NR), the γ is the relaxation constant, E_a , E_b and E_c depend on the incident field polarization. We find that there are one eigenmode with frequency $\sqrt{\omega_0^2 + 2t}$ (with polarization along the central symmetry axis) and two degenerate modes with frequency $\sqrt{\omega_0^2 - t}$ (with polarizations perpendicular to the central symmetry axis) [we have neglected γ for the eigenmodes analysis]. Therefore, we may observe two peaks (one with wavelength shorter than that of the single NR, the other with wavelength longer than that of the single NR) in the scattering spectra, though there should be three modes in general.

The FDTD method is applied to simulate the scattering spectrum of the structure. The length and the radius of the rods are 38 nm and 6 nm. The interface distances among the ends of the NRs are 6 nm for $\theta=90^\circ$, 9 nm for $\theta=60^\circ$, and 12.5 nm for $\theta=30^\circ$, respectively. The background is air. The optical response of the TNR depends on the incident field polarization (relative to TNR). We first consider the case of $\theta=90^\circ$ as an example. Similar discussions can be applied to the cases with $\theta=60^\circ$ and $\theta=30^\circ$. There are mainly three types of contributions to the scattering spectrum. The first type of contribution (we call it type A) to the peak with wavelength longer than that of the single NR

comes mainly from the incident field with polarizations outside the cone formed by the TNRs. The second type of contribution (type B) to the peak with wavelength shorter than that of the single NR comes mainly from the incident field with polarizations within cone formed by the TNRs. The third type (type C) contributes to both peaks. This type of scattering spectrum is mainly due to the plasmonic analogue of electromagnetically induced transparency (EIT), for example from the incident field with direction along one of the NR as shown in Figure S14.

The total scattering spectrum observed in experiment is the summation of the three types of contributions. The type A scattering spectrum is from the fields with the incident angles (with respect to the central symmetry axis) $0 \leq \alpha < 35.3^\circ$, which ensures that the incident field polarization outside the core. We use the scattering spectrum of one typical incident field with $\alpha = 0^\circ$ and the field amplitude proportional to the corresponding solid angle to mimic the type A scattering spectrum. The type B scattering spectrum is from the fields with incident angles $35.3^\circ < \alpha \leq \alpha_{\max} = 70^\circ$ (we have assumed the maximum incident angle to be $\alpha_{\max} = 70^\circ$), which ensures that the incident field polarization within the core. We use the scattering spectrum of one typical incident field with $\alpha = 70^\circ$ and the field amplitude proportional to the corresponding solid angle to mimic the type B scattering spectrum. The type C scattering spectrum is calculated based on the incident direction along the NR. The relative weights of type A and type B scattering spectrum are determined by the corresponding solid angle related field intensity. The relative weight of type C scattering spectrum to that of type B is chosen as 4. Thus, the weights are $0.151A+B+4C$ for $\theta=90^\circ$, $3.20A+B+4C$ for $\theta=60^\circ$, and $A+4C$ for $\theta=30^\circ$. The scattering spectra are shown in the following figures. We see two peaks as predicted by the mode-coupling analysis (Fig. S15). And we have a qualitative agreement between the theory and the experiment. (Note that for the case of $\theta=30^\circ$, the type B scattering vanishes since there is no polarization within the cone for all incident fields with $0^\circ \leq \alpha \leq \alpha_{\max} = 70^\circ$.)

This type of scattering spectrum is mainly due to the plasmonic analogue of electromagnetically induced transparency (EIT).^{S3,S4} Figure S14 shows the scattering spectra of type C contribution for $\theta=30^\circ, 60^\circ, 90^\circ$, where we see clearly dips in the scattering intensity of the spectra. To further clarify the mechanism, we show the near field maps for $\theta=90^\circ$ in S16 (The main feature is the same for the configurations of $\theta=30^\circ, 60^\circ$). In this case, the incident field direction is along Z axis (the long axis of one nanorod, nanorod I) and the polarization of the electric field is along the Y axis. One can see that the incident field mainly generates net dipole moments of the nanorods II and III, which lead to the bright field modes. The near field interaction between the nanorods II/III and nanorod I induces the quadrupole excitation of nanorod I, which forms the dark mode. The interference among the fields from bright

modes and dark mode leads to a dip in the scattering intensity of the spectra. This plasmonic analogue EIT is similar as that in the T-shaped nanorod dimer.^{S5} In general, the angle among the nanorods (θ) and the distance between the ends of the nanorods (d) have impact on the dip in the scattering spectra. Our calculations have also shown that the dip becomes deeper with decreasing the inter-nanorod end distance d (i.e., increase of the interaction among the nanorods) as shown in figure S17.^{S4}

III. Supporting figures

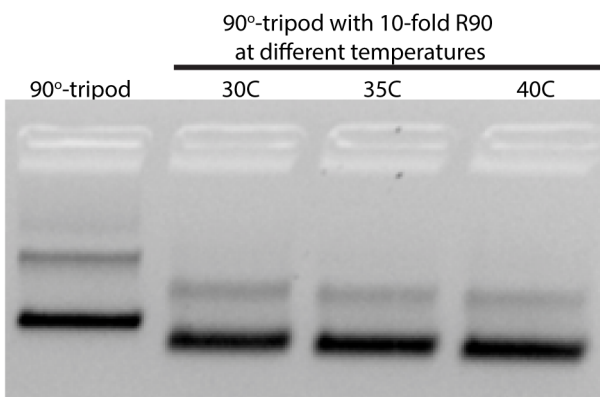


Figure S1. Agarose gel electrophoresis image of 90-90-90 tripod (90°-tripod) treated with 10-fold excess of R90 (releasing strands) at various annealing temperatures (at 30°C, 35°C and 40°C) for 4 hours followed by keeping at room temperature for overnight.

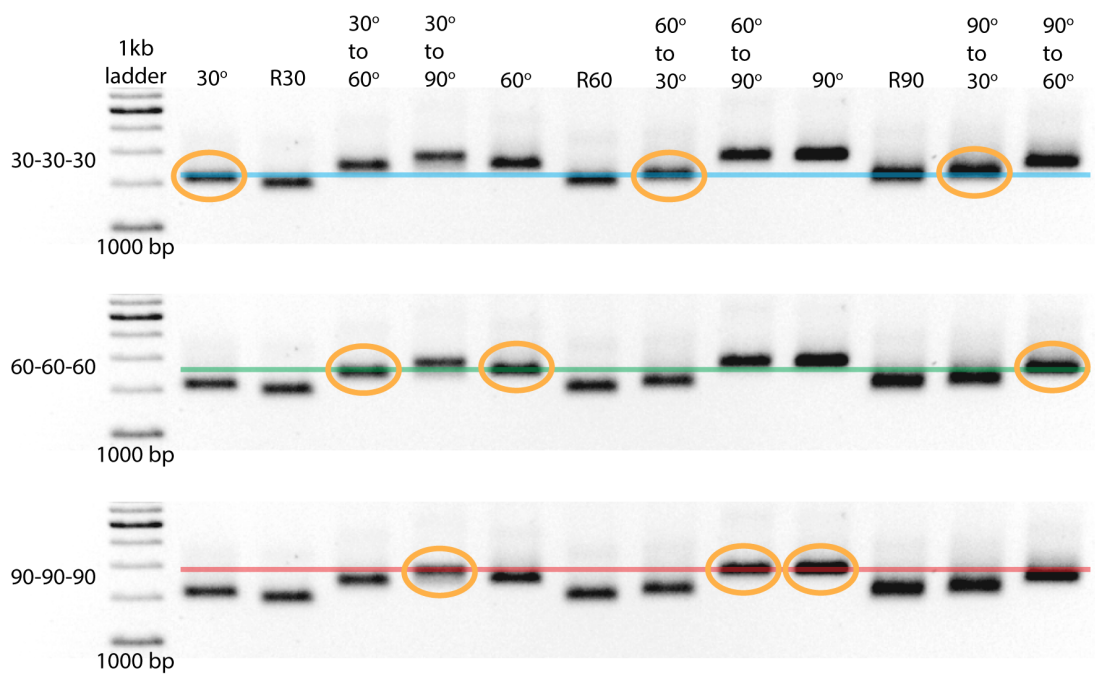


Figure S2. Agarose gel image showing conversion of one tripod conformation to the other two conformations. Here same gel image is presented three times to highlight individual tripod conformations (30°, 60° and 90°). Bands R30, R60 and R90 correspond to the released conformation (no locking state) from 30°, 60° and 90°, respectively.

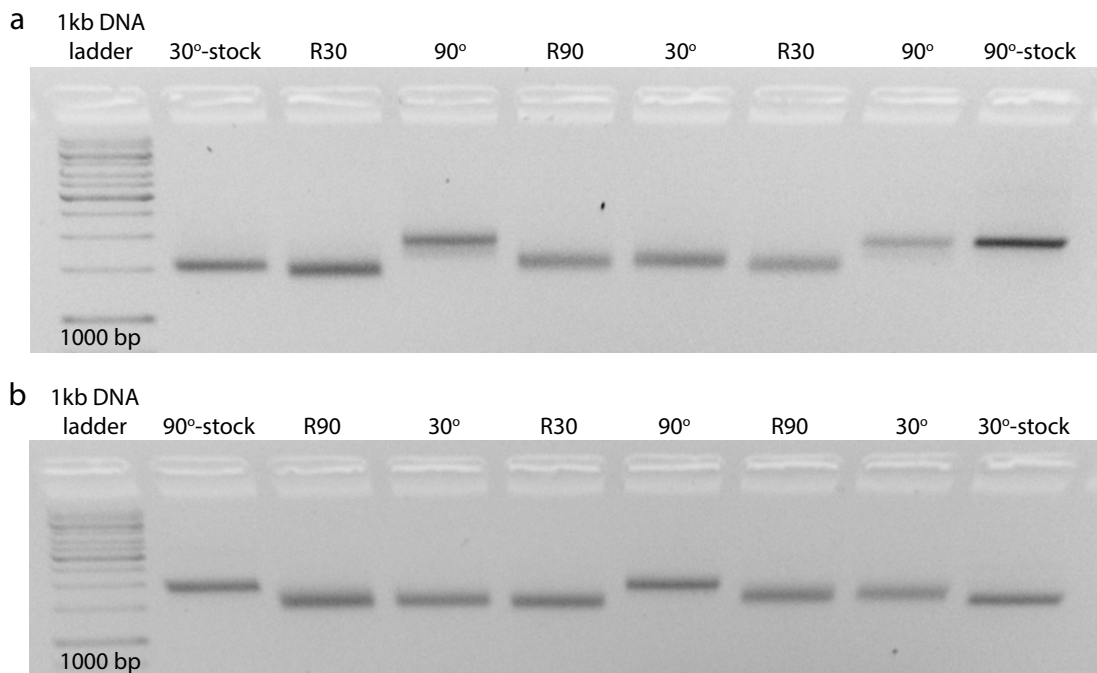


Figure S3. (a) Agarose gel electrophoresis image showing back and forth conversion of 30-30-30 tripod (30°) to 90-90-90 tripod (90°). The bands for R30 and R90 correspond to strut released conformation (no locking state) achieved from 30°- and 90°-tripod, respectively. (b) Agarose gel electrophoresis image showing back and forth conversion of 90-90-90 tripod (90°) to 30-30-30 tripod (30°).

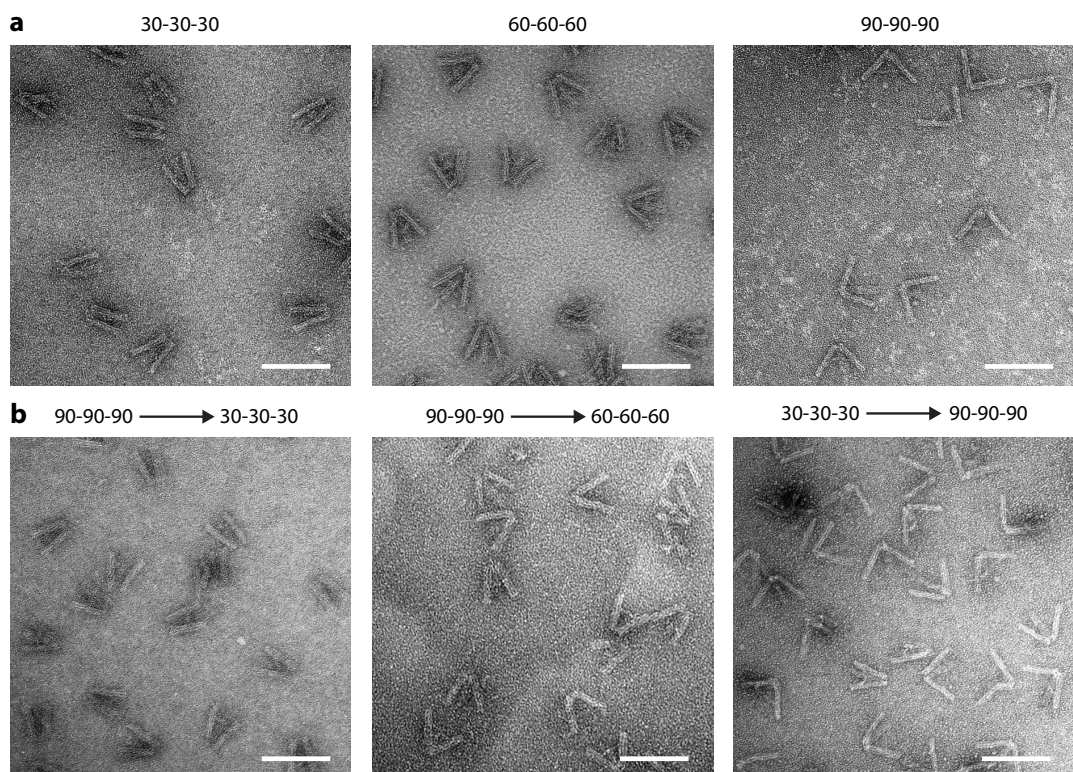


Figure S4. (a) TEM images of 30-30-30, 60-60-60 and 90-90-90 tripod. (b)

TEM images of 30-30-30 converted from 90-90-90, 60-60-60 converted from 90-90-90 and 90-90-90 converted from 30-30-30. Scale bar, 100 nm.

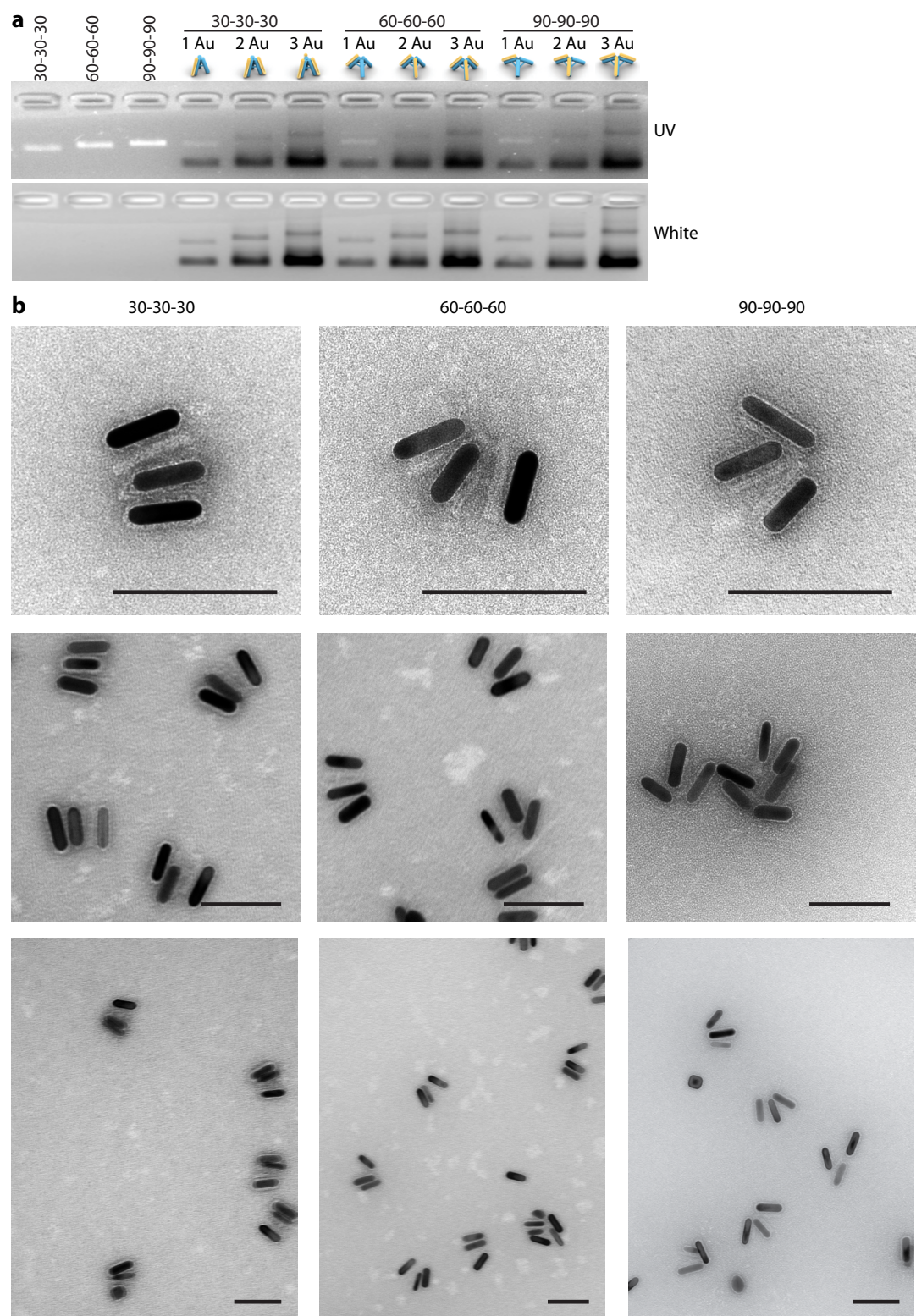


Figure S5. (a) Agarose gel electrophoresis image (UV and white light illuminated) of tripods with one, two and three AuNRs. (b) TEM images of tripods with AuNRs. Scale bars, 100 nm.

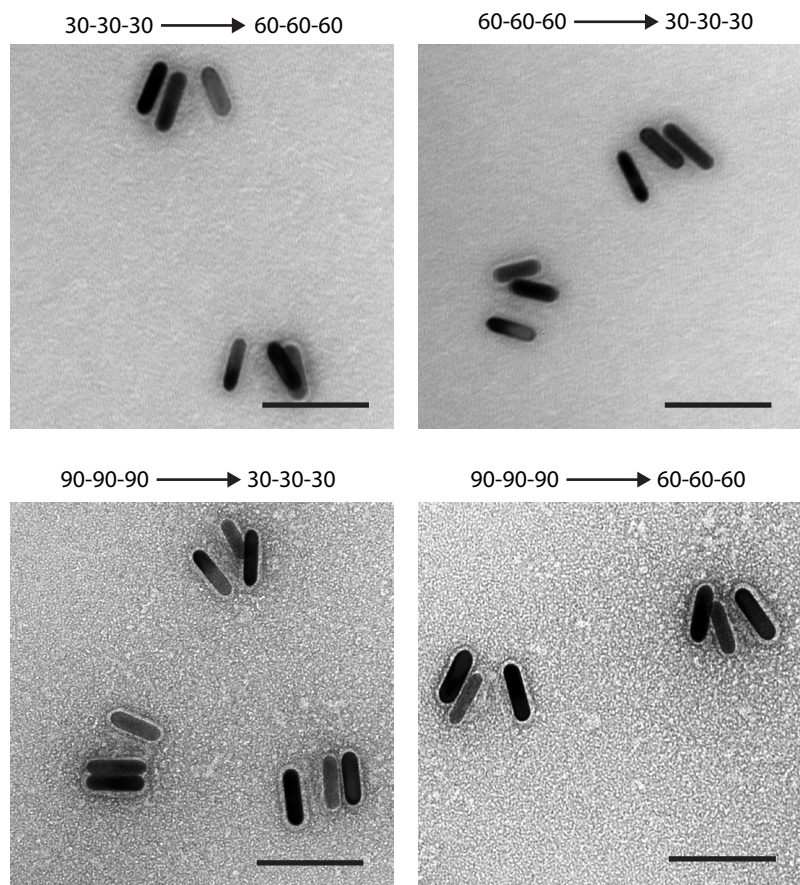


Figure S6. TEM images of 60-60-60, 30-30-30, 30-30-30 and 60-60-60 converted from 30-30-30, 60-60-60, 90-90-90 and 90-90-90, respectively. Scale bars, 100 nm.

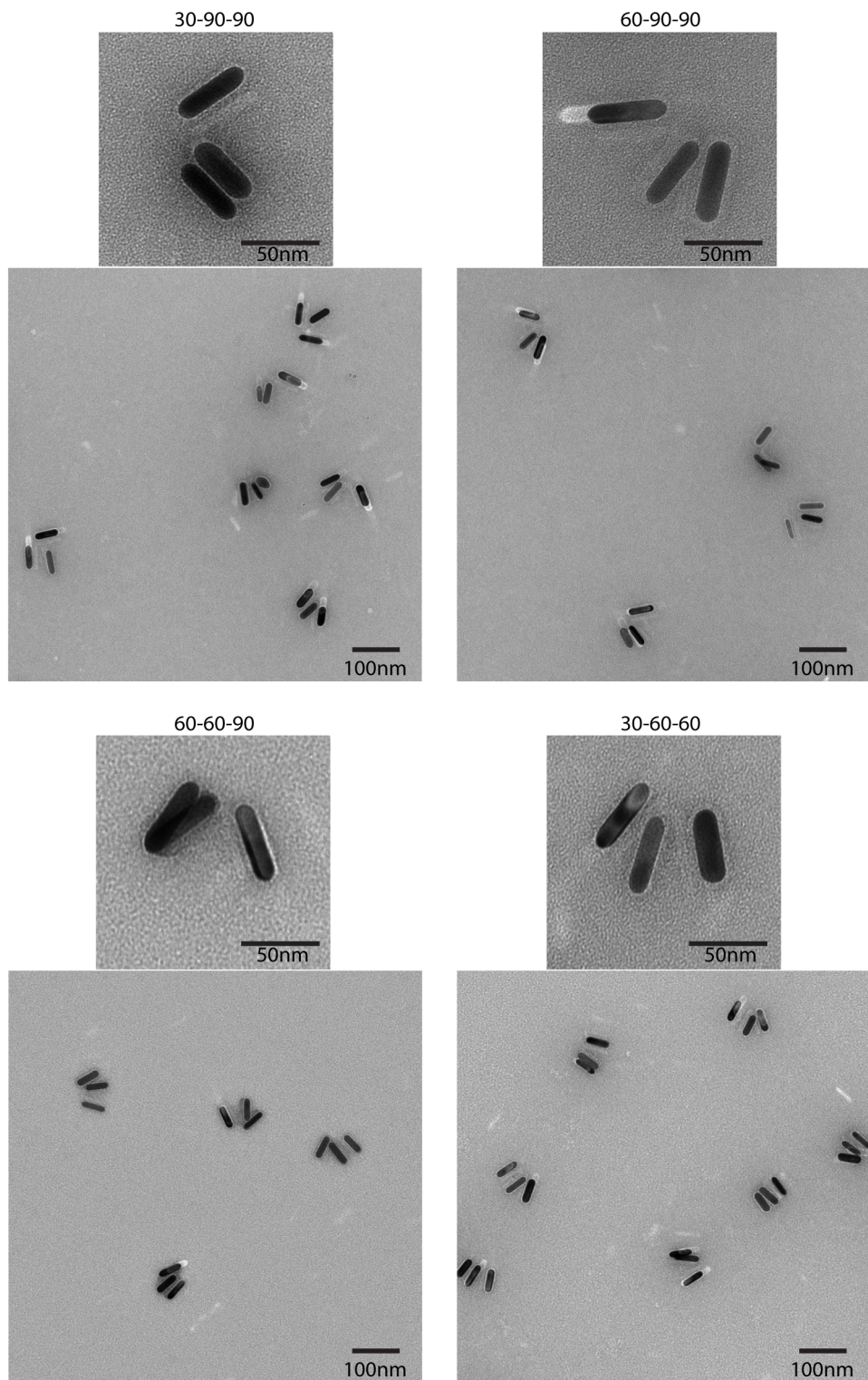


Figure S7. TEM images of AuNR conjugated 30-60-60, 60-60-90, 30-90-90 and 60-90-90 tripods.

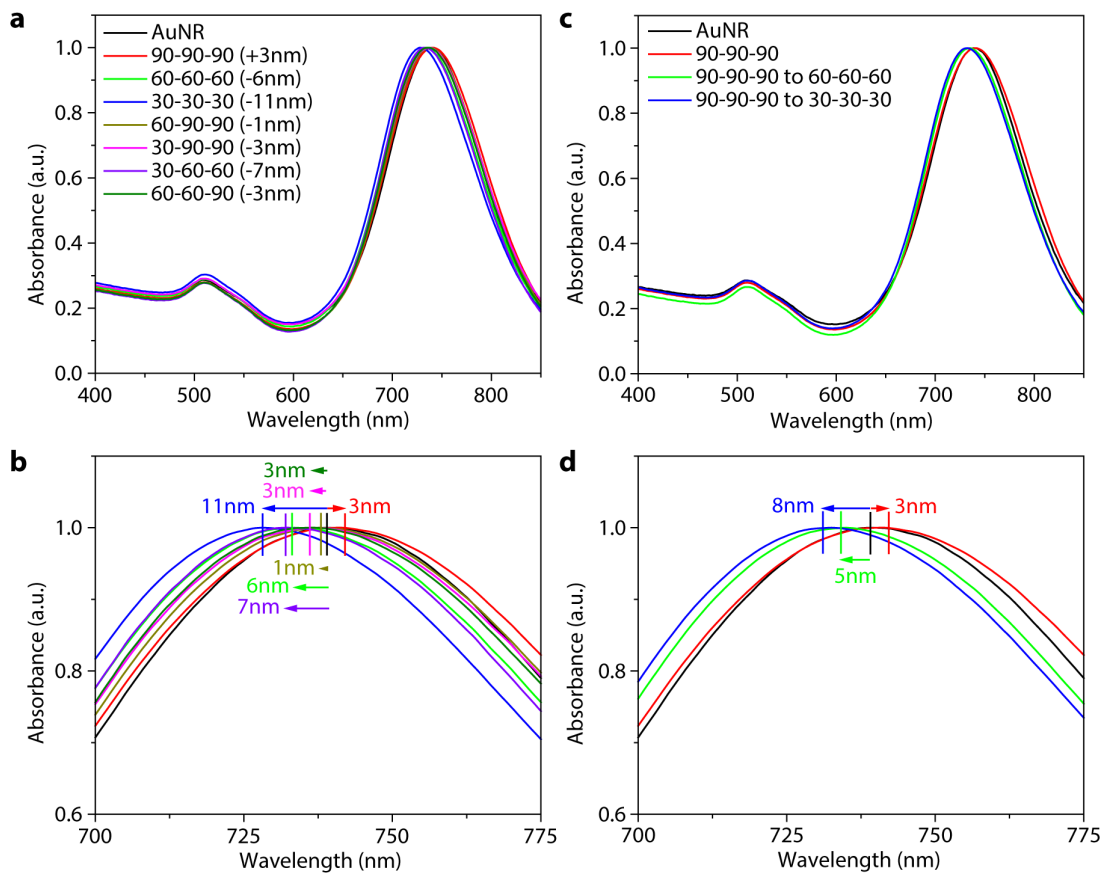


Figure S8. (a) Absorbance spectra of free DNA conjugated AuNR, and AuNR modified 30-30-30, 60-60-60, 90-90-90, 30-60-60, 60-60-90, 30-90-90 and 60-90-90 tripod with corresponding LSPR peak shifts. (b) Zoomed in spectra of (a) showing LSPR peak shifts of various tripod conformations compared to free DNA conjugated AuNR. (c) Absorbance spectra of free DNA conjugated AuNR, AuNR assembled 90-90-90 tripod, and 30-30-30 and 60-60-60 tripod converted from 90-90-90 tripod. (d) Zoomed in absorbance spectra of (c) showing shifts in absorbance maxima.

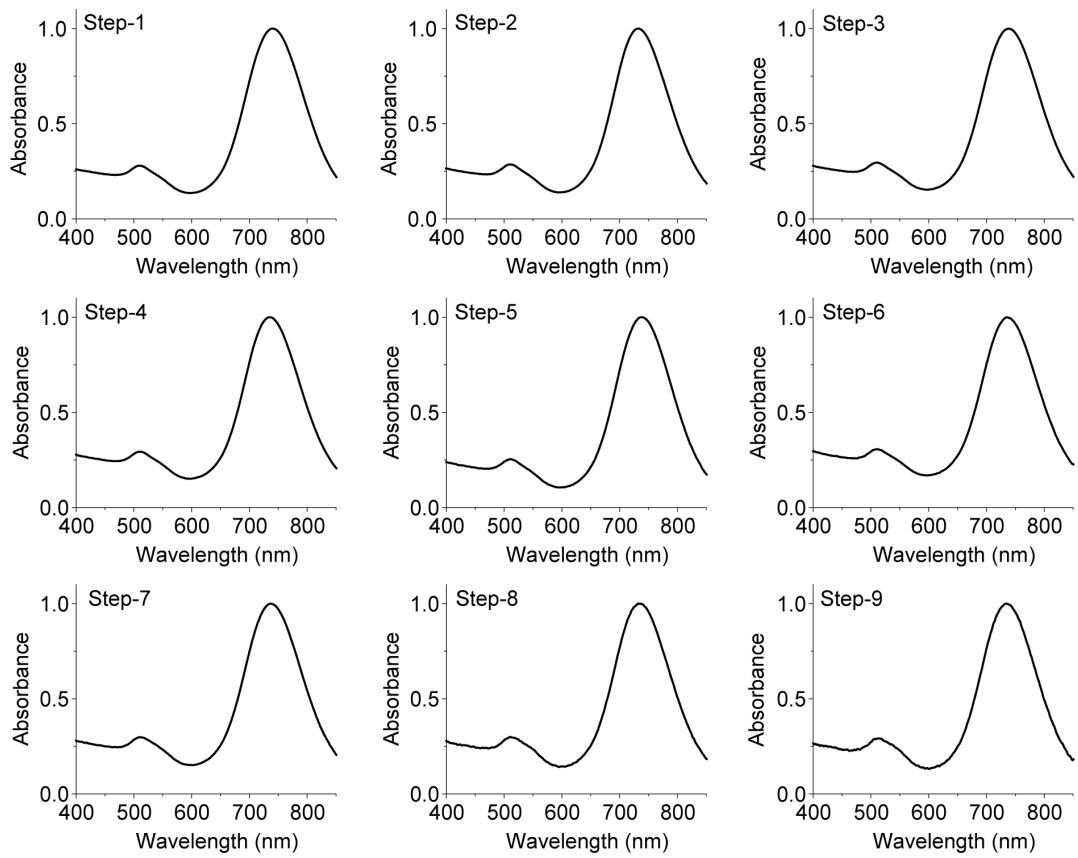


Figure S9. Absorbance spectra of each steps from reconfiguration cycle experiment (Figure 3f). Step-1 corresponds to 90-90-90 tripod (red sphere, Figure 3f).

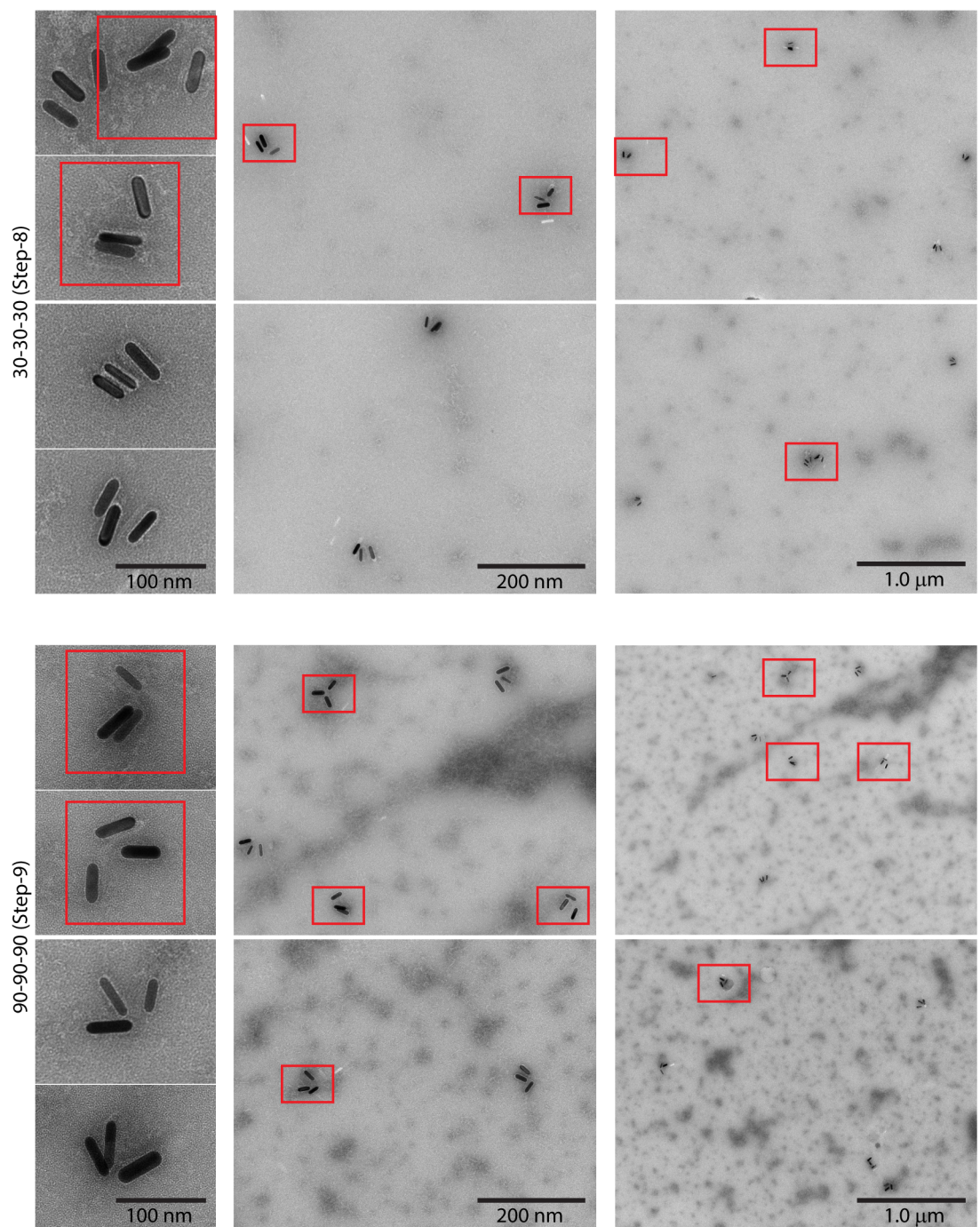


Figure S10. TEM images of the 30-30-30 AuNR-tripods from Step-8 and the 90-90-90 AuNR-tripods from Step-9 from reconfiguration cycle experiment (main text Figure 3f). Some of the partially transformed AuNR-tripods are highlighted with red boxes. Images of the 30-30-30 AuNR-tripods from Step-8 show that some angles are larger than 30°. Similarly, images the 90-90-90 AuNR-tripods from Step-9 show that some angles are smaller than 90°.

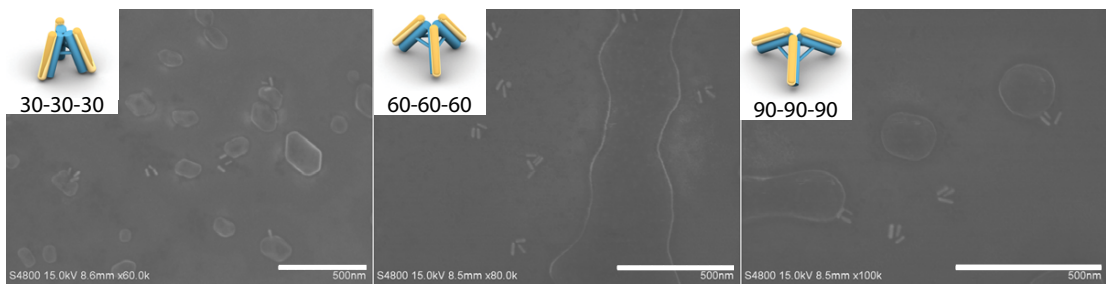


Figure S11. Additional SEM images of AuNR-tripod nanostructures without biotin modifications. Scale bar 500 nm.

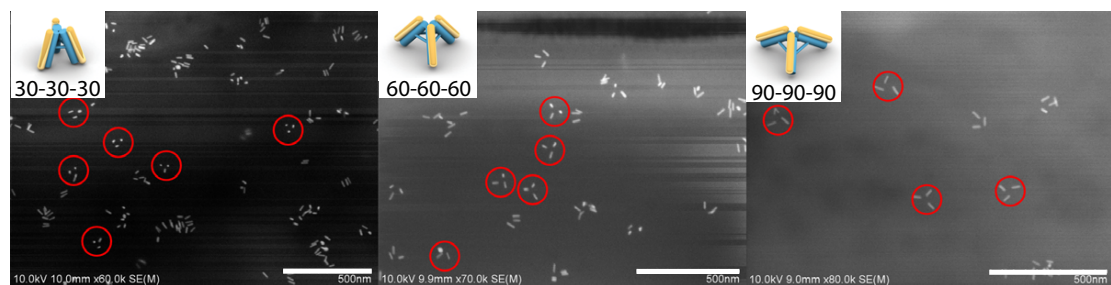


Figure S12. Additional SEM images of AuNR-tripod nanostructure with biotin modifications. The AuNR-tripods show stand-up configuration on streptavidin modified substrate due to the biotin-streptavidin interactions.

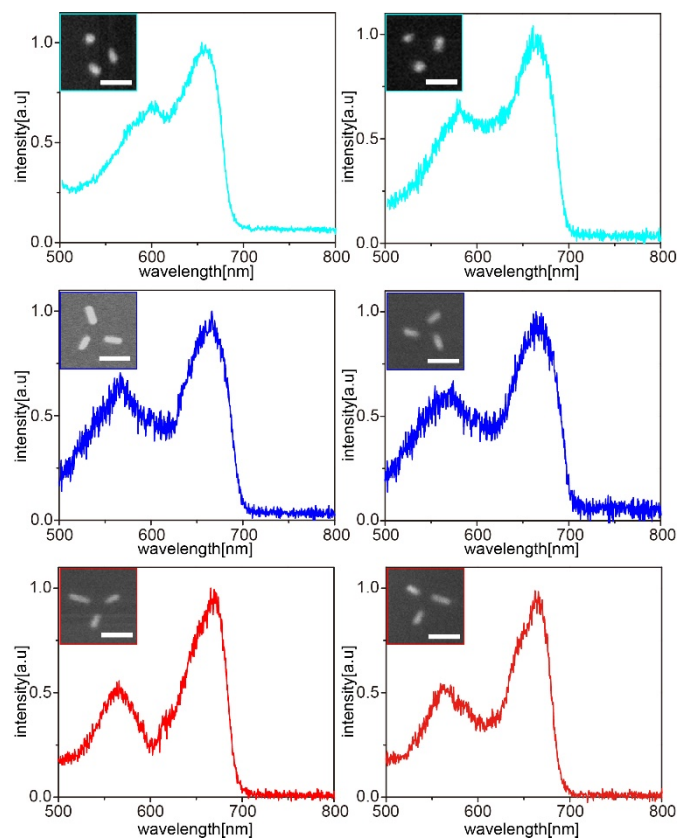


Figure S13. Additional light scattering spectra for individual three AuNRs arranged (top) in a 30-30-30 configuration, (middle) in a 60-60-60 configuration, (bottom) in a 90-90-90 configuration, all on silicon wafer and in air. Insets in

left-side show the SEM images of the particles giving rise to each scattering spectrum. Scale bar = 50 nm. Insets in right-side show the designated configuration for simulation, the size of AuNR is ~38nm \times 12nm.

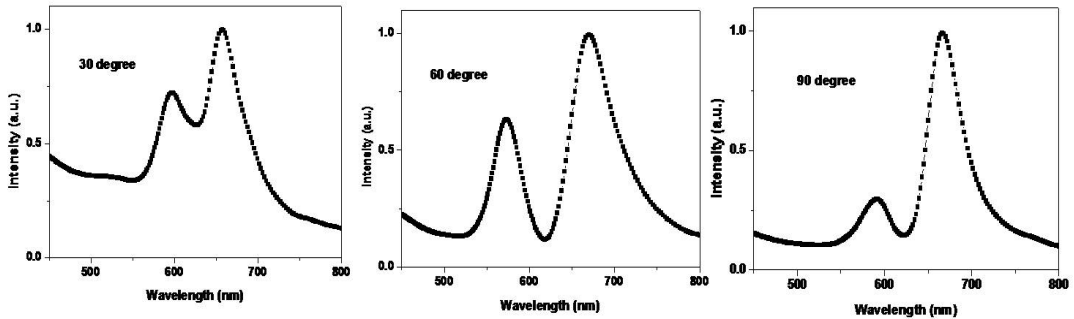


Figure S14. The scattering spectra of type C contribution for $\theta=30^\circ, 60^\circ, 90^\circ$.

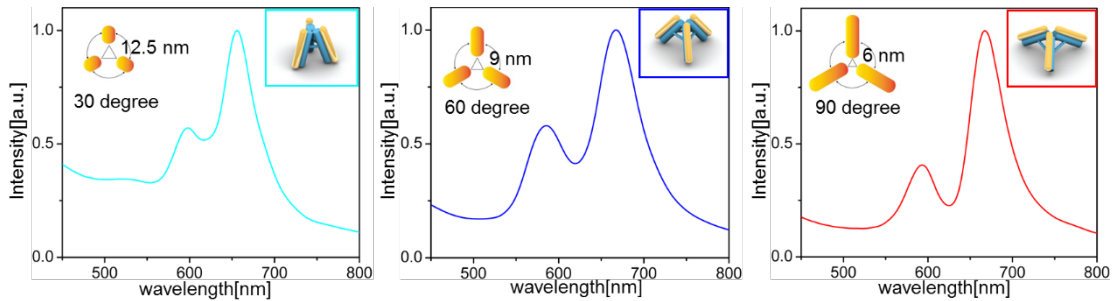


Figure S15. The normalized scattering spectra of the TNRs for $\theta=30^\circ, 60^\circ, 90^\circ$. Notes on calculation details: The cone angle 2α is calculated by the formula $\alpha = \arcsin(2 \sin(\theta/2)/\sqrt{3})$. For the case of $\theta=90^\circ$, the cone angle is $2 \times 54.7^\circ$. Then the incident field angle should satisfy $0 \leq \alpha < 35.3^\circ$ to ensure that the incident field polarization outside the core. The solid angle corresponding to the cone angle 2α is calculated by the formula $\Omega = 2\pi(1 - \cos(\alpha))$.

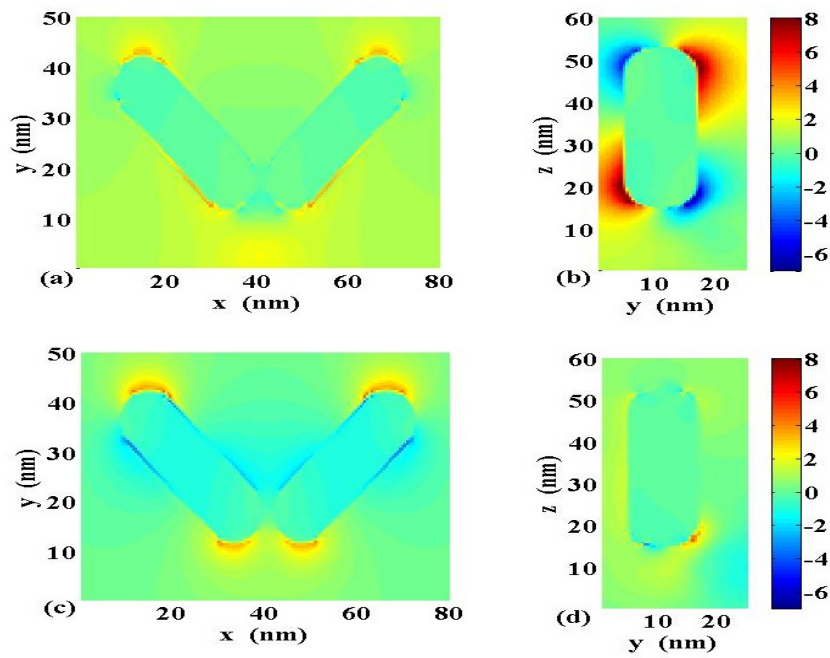


Figure S16. The near field distribution of $\text{Re}[E_y]$ ((a),(b)) and $\text{Im}[E_y]$ ((c),(d)) for the case of type C with $\theta = 90^\circ$. The wavelength of the incident field is 620nm.

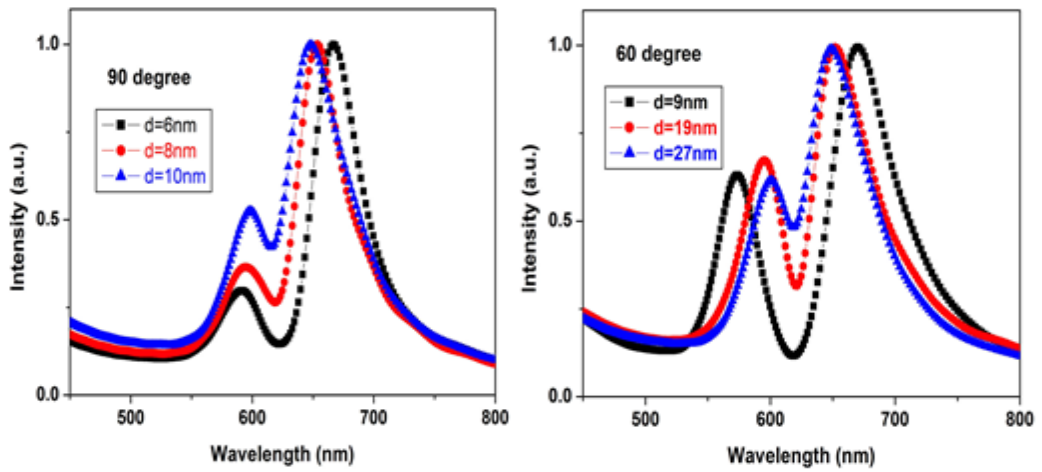


Figure S17. The scattering spectra of type C configurations for $\theta=90^\circ$ ($d=6\text{nm}$, 8nm , 10nm) and 60° ($d=9\text{nm}$, 19nm , 27nm).

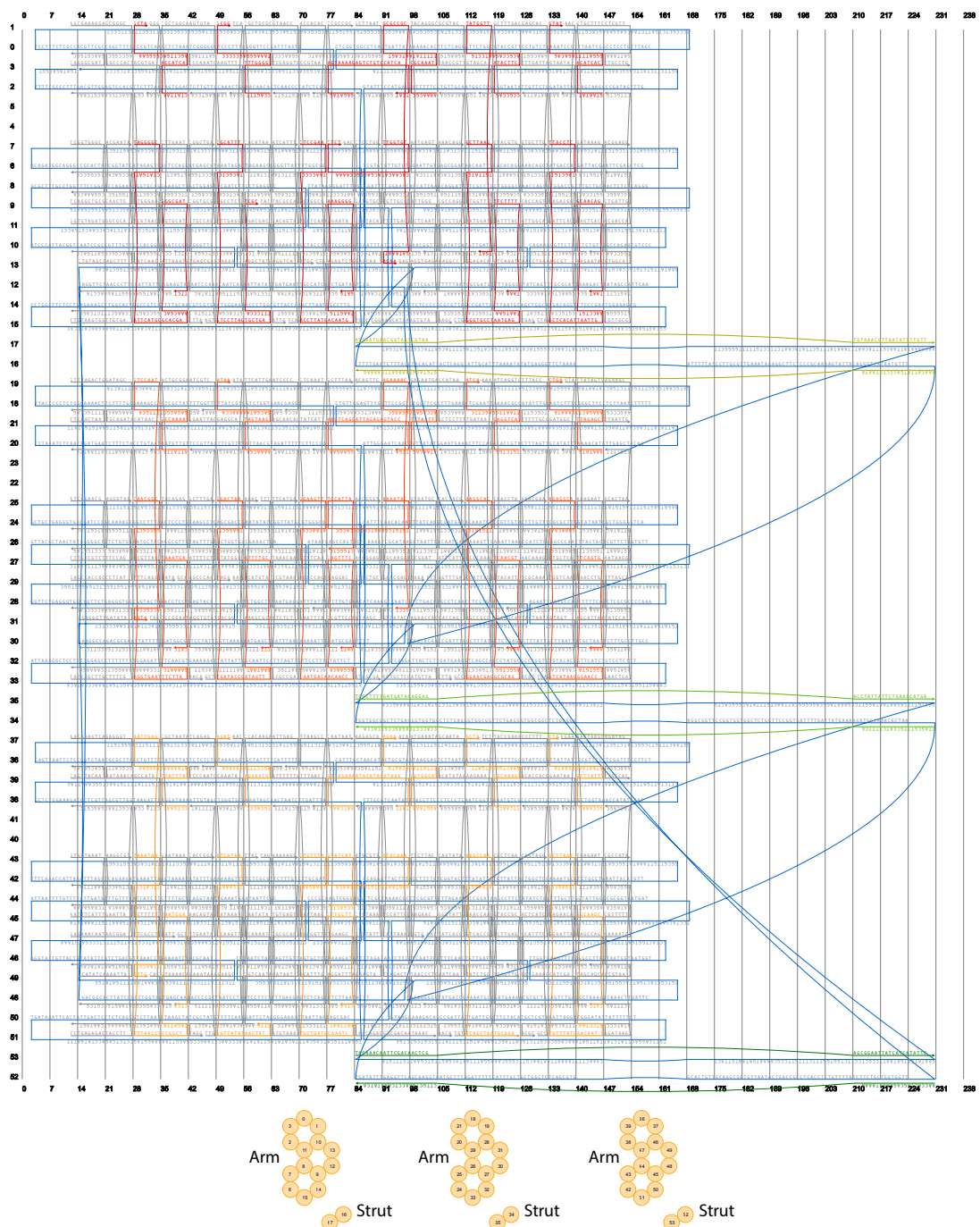


Figure S18. Strand diagram of 30-30-30 tripod.

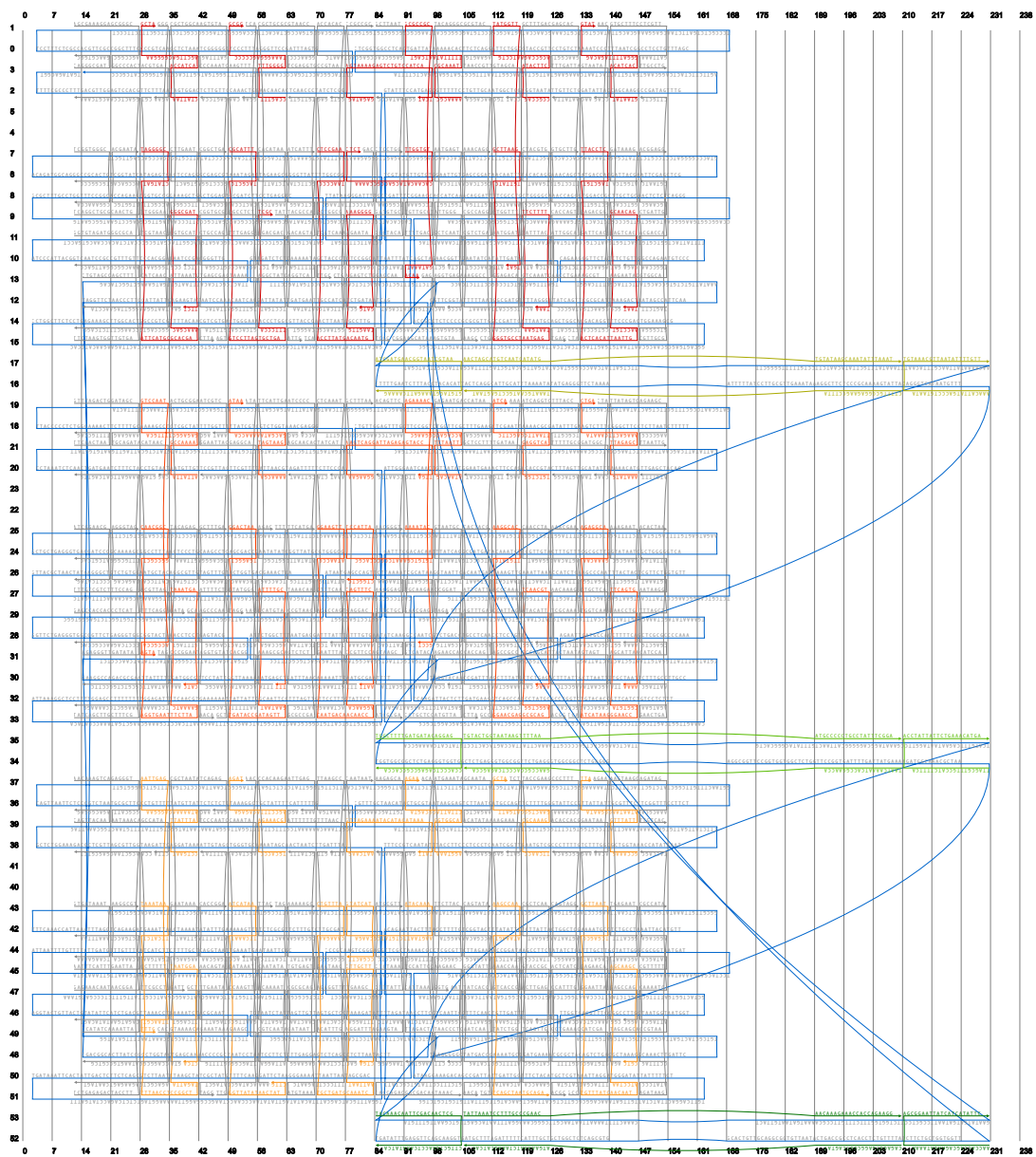


Figure S19. Strand diagram of 60-60-60 tripod.

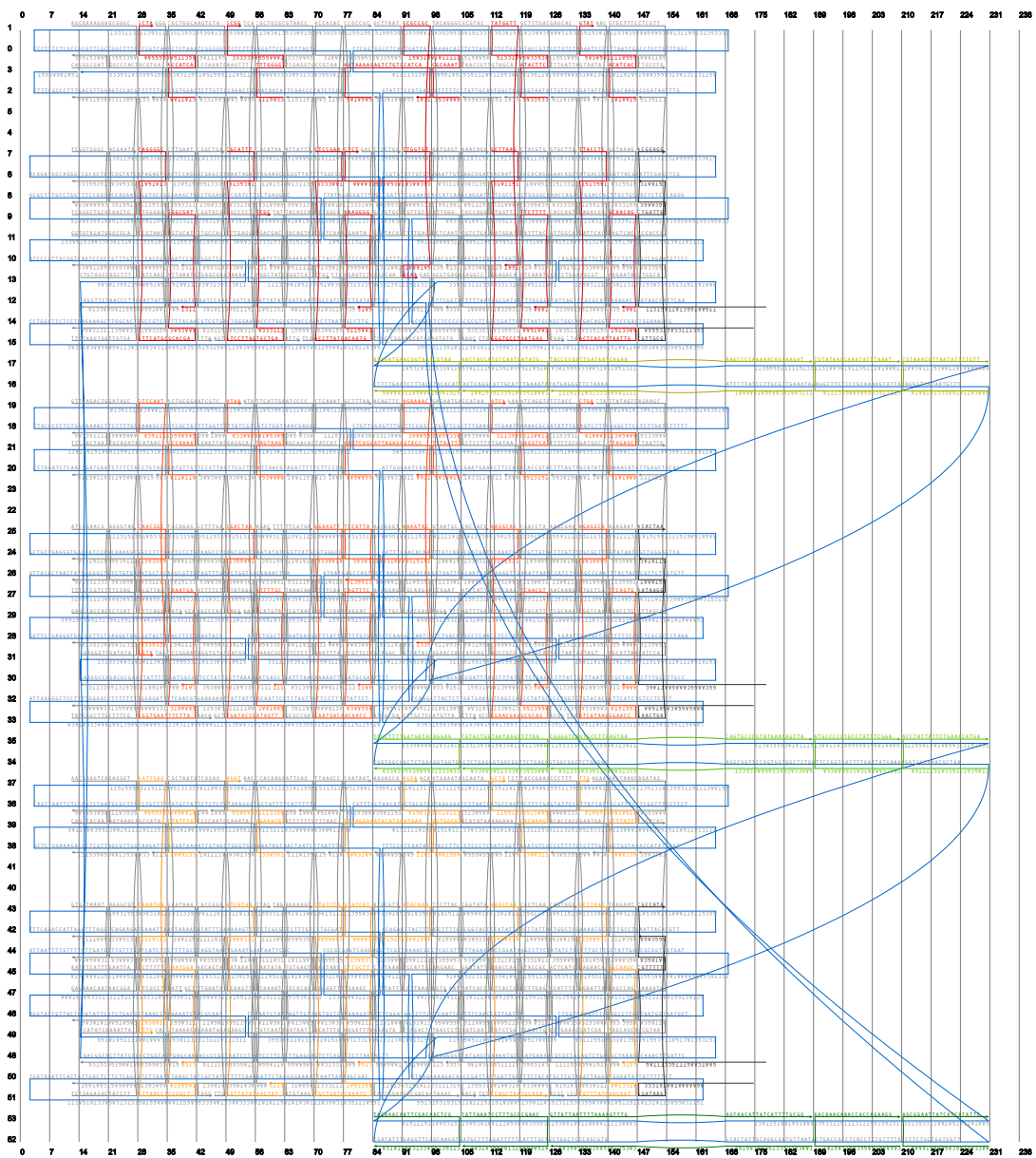


Figure S20. Strand diagram of 90-90-90 tripod.

IV. DNA Sequences

core-1	GCAAGAGTCTGGAGCAATAATGCCGCCTACAAATACCC
core-2	GCGAAGAACATCGTGGCATGCCAACGACCACTTGCTG
core-3	GATGTGCTTCCTCGTTGATTAAATTGCCTG
core-4	ATAGCTTGACGAGCACGAACGGTTTGATTAGTAATACCAG
core-5	AACAGGTGAGAAAGGCCAACCGTCGTCTGAAACAGGA
core-6	ACAGTCAAATCAACCTGAAAGCGTCGAAC TGATAGCCCCACCAGTTGCCAGTGCTTG
core-7	TCAGCTTCTAACTATTACACATAAAAGATCGGGACGACGAGA
core-8	CGGAAGCATAAAGTAGGGAGAGGCGGTCAAGGCGATT CGC
core-9	CTGCGCTCACAAATTCCAATGAGTTGGTGGT GCTCAATTCTA
core-10	CTATT CCTGTGAAATCTACGTGGCAGGCGTATTTACATCA
core-11	GAAAATTAAATGTGAGCGAGTAAATGTTGGATTATACCGGTGCGGCCAGCTCGGCTGA
core-12	GAGGCTGATTATCAGATGATGTGCTCGGCAACTCCTGG
core-13	CTGATT CATCAATATAATACGCCACCTCAGGATCATTT
core-14	AGTGCCCTGGAGTGACTCTGAATT TCGGCCGTGCATT TCT
core-15	TTCTAAGTGGTTGTGAACCGACAGTGC GGCCC
core-16	TTCCCATTAGTAATCATAACCCAAACTGACCTTCATCAACTTA
core-17	CGTTCGAACACCGCTTTGGAAAGGCCAGTGCAAGCTT CTCAGG
core-18	CAATTGAGGC ACTCCAGGCCCTGTCA CGAC GTTGTACTTA
core-19	ACAGTTCAAACCTCAACAGCCCTCGTTCTCAAATTAAA
core-20	AAATTGAGGCAGCCGCCAAAGCTAAATCGGTATTCA TTGTGAATCACTACG
core-21	CTAGGCATCAATTCTGATGCCAAAAGTACGG
core-22	AGCGGAATTACGAGGCAACTAACGTAGG
core-23	GGGTGGGAACC ATCAACTAATGGAAGGGTTAGAACCTA
core-24	TCAACCAACCCGTCGGACTGCCAGGAGTCCA
core-25	G TAGTT CAGGCATTCCAACGTTAGTCCAAAAAAAAGGCTCCAAAAGG
core-26	ATTGGAGACATGCCATTAAAATGCCAGGTGTTGAAAACAGG
core-27	GCTTACAGGGCGCGTACAGAAGTGTAA CC GTTGTAGCACC AT
core-28	CTAACACCAGTCAGGACAAACAAAGCTTAA
core-29	TCTCGCTGCCGTAA CGGAACCCCTCGAGGTGCCGTAA GGTT
core-30	TTCGAACAGTGC GATT TGCAAGAACCGGATTGTA
core-31	CCCGCGCTGGCAAGTGTAGATTAGCCAAATCAAGTTGGAA
core-32	CTGTAGCCAGCTTAAACGGCGGATTGACC
core-33	GGTGTAGATGGCGCAGGACTCCAACGTCAA
core-34	TAATGGTCAAGAGATGGCTGCTCACAGACCAGGCGCATACGG
core-35	TATT CCTGTAGGCTATCAGGTCA TTGAGACAGTATGTTGTT
core-36	ATCGGAACGCCCTCATAG
core-37	TCAGGCTGCCAACTGCTGGTGCACGAATA
core-38	ATGGTCAGATAAAGGGTCCACCAAGTCACCA
core-39	TTTCACCAGCCATGTAAGCCAGATTCA TTGAATCCCCACCA
core-40	GACAATCCCTATAAGGGCTGGCGGTAA CGCCAGGTATTG
core-41	TCGGTGGCGGAAACCA
core-42	AACGATT CACGCTGGTTGAGACGGCGTGCCAGTGCATTGAG

core-43	TGCAATGGATAAAATCCGTGGTTTCGGCCAACGCGCGAAGC
core-44	CAAGCGCAAAGAATTGGGCTTAAACCTGAAAA
core-45	ATTATTGCTTCAAACTAAAGGAATTGCGCGCCGAATATATTGGTCGCAGAC
core-46	TTTGTGCTTCCAGCAGACAGAGGGTAG
core-47	GAGGCCACCACCTCATAAAGATTCATCAGTTG
core-48	AGCGAAAGGAGCGGGCAGCCGGGCCACTACGTGAAGAA
core-49	AACTACAAACGTATGGAATTTCACGTTAACAA
core-50	TTTACGATTGAGAATGACCATAAAAGCGAGCTCCTTGATAAAAAGT
core-51	TCCGAATTAGTTAAATCAGCTCATAAACAAAGTTGTTCATGA
core-52	TGAGTCATACAAAAATTGCGATTAAGCGAGTTAACGAAACGGGT
core-53	AGGATCAGGTCTTACCTCGCTTTTGCGGATGCCAAC
core-54	GGTTTATAGTCAGAAGCAAGGCCGTTAATTG
core-55	AGAGGGTTGATATAACCCCTCAGAACCGCCAC
core-56	TAGAATAATTGCGTCTGGCCTTC
core-57	AAACCCGGAATAGGTATACGGACCAATAGGAACGCATTCTACAACGGCTTGAA
core-58	TTTAAAAGCGCAGTCTCTTCACTAACCGTAACCGTTAAT
core-59	TTTCCGTTCCAGTAAGCTATTACGTTCTGCCAACATTG
core-60	CCAAGAACCAACCAGAGGTCAAGGTTGAATTCCAT
core-61	CATGCCAGCATTACTAATAGTAGCTAGCAATAAGCCTAACAAAGTTAACGAA
core-62	TTAACGCATTAACATCCACGAGCTGTTAGCTATGTTT
core-63	GGATTGGACTCCGAAATGTTGCGTATTGGGACCG
core-64	GAGTCATAAAAGAATAGGAGAGGCCGCC
core-65	TATCAGCTGCTTCGTTGCGGGATCGTCAC
core-66	GCTTGCAGGGAGTTAAATACAGAGCCTGTAGGATA
core-67	CCTGCTCCATGTTAGAGTAATCTGAAGAATAGAAATCGCGA
core-68	GCCATCGCCTGATAAAATGTAATGCTACCTTATAGA
core-69	TCAAGTACAACGGAGATCAACCTATCAACTTACATTACATTGAG
core-70	GCTTAATGAGGCCACCGAGCACTAAATCACACACGTAGCTATTGC
core-71	CAGGGCGATGAACGTGGC
core-72	AACAGAACCTCTGCCATTGGCAAATATTA
core-73	GTTTAGACTGGATAGCAAAGAAGTGCAGATAACAAACAG
core-74	ATAATCGTACTCAGGAGAGGCCAACAAAC
core-75	TTCAACTAATTGCGCAG
core-76	AAACAAAGTCAGAGGGTGCACATTAATAAACAGCCATACTTA
core-77	AACGAATTGCGTAGATTTGAATAATTAT
core-78	AAGAGCATGTTAGCAAACGCAA
core-79	ACATTATCTATTAGACTAAAGTAT
core-80	TCTGTTGAAATATCTGGATTTCGTCATAGGGTATTAAGAACGCAGTATA
core-81	AGAAAAAACGTACCAAAACCATTTGGCGACA
core-82	AACTCCCAATCCAAATAAGCTACACCAAGTTAATT
core-83	AGCATTGTTAACATTA
core-84	AAATGATTAAGCCGCACTAAACATTGTCCTCAA
core-85	CAGTTACAAAGACGGGAG
core-86	CCATTGCGCTTGATGAACCTTTAGACGCTGAGAAGAGTCATAGT

core-87 GACAGCAACACTATCATAAAT
 core-88 GCAGTTAGTACTGCGGAATCGTCAAAT
 core-89 GTTAGAGGTTTGAAGCTTTAGGACAATAAT
 core-90 CCATATCAAATTACAGATGAATATACAGT
 core-91 GACCATTAAATTTAGCTCCATTCCAAGAACCCCC
 core-92 CACCCAGGCGATAAGTGCCGTG
 core-93 GAGGTACCGGTATTCTAACCAAATCAATAATCGGCTAAC
 core-94 GCTGAAACCATCGACTGTAGCGCTTTACTCATCAGAAGGCCAGTAGG
 core-95 AAGGGATTACAGATATGAGAACATTACGAGCATGTAACGC
 core-96 GTAGTAAAACAGAAATAAGAAGCTTAGCGGGTTTGAACAGTATGAGAACACCGGA
 core-97 GTGATAAATTCAAGAAAA
 core-98 GAGAAGGTGTGAGTGAATTATAAAAAGC
 core-99 ACATACCGAAGCCTTCCAAAAACACCACGGAATAACAA
 core-100 TAGTCATTCACAAAATTAGATTACCACAAGAATTGAGAAAT
 core-101 GCCAGTAATAAGAGAACGCTCAATTATCGACTTGAGATCA
 core-102 TGTACCGACAAAGGTATTCTTACCGAGGCAGGGT
 core-103 TTGATATTTAGTTAATGAATAAAAAGAAGAGATT
 core-104 TCTGAGAGACTACCTTCTGACCTAAATTAA
 core-105 GGCATTTGAGAATAGCAAATGAGCCAGAGGC
 core-106 ACCCATAAAATACATAGCGATAGCTTAGG
 core-107 GCGGGGCGAATAACTTCCCTAGAATCATGTAACCGCAGAAAACCTTTAC
 core-108 AATTCATTTGAATTAACAAACAAAGGCGT
 core-109 GAGAAACAATAACGGAACGCTAACGAGCGTCT
 core-110 GCTTCAGGTCGCTAATATCAGAGGAAT
 core-111 AATAGGAAGGATGAAATAGCAATAAAGACTCACATATAAAAGAAAGATT
 core-112 GTCTTCCTTATGTCGCTATTCAACAGACGACGACAATAAAC
 core-113 CGGAAGTAAGCAGATAGAACGCATTGTCAC
 core-114 GACAGGATTTAGAAGTAAAATCCTTATTGGAATA
 core-115 TAAGAGGCTGAAAGAACCTCATGCGTT
 core-116 GAAACCAGTACCGCCATCGGCTCAGTTG
 core-117 AGATAGCAGCACCGTAAATTAGCACAAATCTACCAGC
 core-118 AAACAATATAATTAGGACGTCAATAGATAATCAACTAACGCGCAGGCTATTT
 core-119 CTTAACCCCTCAATCAAGGAATTGTATCACCGGAGGG
Biotin binding handles
 Handle-bio-1 TCTCTCTCTCCGCTTCCAGTCGGACGTTGCGCGTAATC
 Handle-bio-2 TCTCTCTCTCAGAAAAATAATATCCCAGATAAGAGGCAGA
 Handle-bio-3 TCTCTCTCTTGAATGGCTATTAGTCTGATTGAGCAAGCACGGAGG
 Handle-bio-4 TCTCTCTCTCGAATCAAGTTGCCTTACGCTTTAATAGCACGCCATA
 Handle-bio-5 TCTCTCTCTCGGCAAGGAAAGAATTAGCAATAAGGAGTAAATACACTAA
 Handle-bio-6 TCTCTCTCTCAAAGAGGACAGATGAAGAACTGAATTATAC
AuNR capturing strands
 handle1-1 AAAAAAAAAAAAAACAGTTTTGGGTAAAGGGAGCCCCCGCG
 handle1-2 AAAAAAAAAAAAAATTACCTCTAGCTGACTCACATTAATTGAACCTGTGCAACAGTAAT
 handle1-3 AAAAAAAAAAAAAACGCATTACGCTCGCCTTAGTGTGATTCCATCGC

handle1-4	AAAAAAAAAAAAAATAGGGCCTATGATATTGCGCACGAAAACGACGGCGATTCT
handle1-5	AAAAAAAAAAAAAGTAATATACATCACGGGATTTAGACAGGTAT
handle1-6	AAAAAAAAAAAAACGCCAGATACTTCAGCCAGAACCTGTATGGTTGAT
handle1-7	AAAAAAAAAAAAAGCTTAAGTGTATCGGGGCCATTAGACTAATGAATTCTTTAAA
handle1-8	AAAAAAAAAAAAAGAGATAGAGTAAAGAGTCTGTCCATCATCAT
handle1-9	AAAAAAAAAAAAACGCCAAATTTCATAATCAGTGCGCCGCGATAAACAA
handle1-10	AAAAAAAAAAAAATTGGTGTCAACACATACGACGCCAAACTCT
handle1-11	AAAAAAAAAAAAACTCCGAATAACCCCACCTTATGACAATGTAAGTTGAAAGGGGATG
handle1-12	AAAAAAAAAAAAACTATTAAACCATCAAGCTTGACGGGGAGCTA
handle2-1	TAATAATAATAATAGGAAGTTATAACCGCAATGACAACAAACAGGAACAGTTCAATT
handle2-2	TAATAATAATAAAACGATAGTAAGGACGATAAAACCAATAA
handle2-3	TAATAATAATAAAAGGAGGCAGAAACAAATCATAGGGAACCCGGTATTAGTGA
handle2-4	TAATAATAATAAAATTATTAGCCAAAGAGAGGGCTTGCAGTCAAACCGCCAAGTA
handle2-5	TAATAATAATAAAAGGCACTGTATCGGAACGAGGCCAGAGGCTGGTCAACGTAGAG
handle2-6	TAATAATAATAATAAACAGTTAATTACAGACCGGAAGCAGAACAGCCT
handle2-7	TAATAATAATAAAACTGTGTGCAAATCCGCCACGCTCCATTACTGGCTC
handle2-8	TAATAATAATAATATGTCTGGAGGTCTTAATTGAGCTTCATCA
handle2-9	TAATAATAATAAAATATGTTAGAGCAAAGACTCAAATACTGA
handle2-10	TAATAATAATAACCGGCCGCTAGGTGAATTCTTAGAAAATCTAAATGACATC
handle2-11	TAATAATAATAATAGGAAGAAAAGTCAGGATTAGAGAGTACCTTGA
handle2-12	TAATAATAATAATAGGACTAATGAGGCTTGATACCGATAGTTGAATAATATTTGCTT
handle3-1	AGGAATAGTTATAATGCACCCAGAACGAGCCTTACAGAGAAGAT
handle3-2	AGGAATAGTTATAACCTGAATTATAAAAAACAGGGAAATTGAGTTAACGTTT
handle3-3	AGGAATAGTTAAAGGTAAAGGTGGCACTTATTACGCAGTAAGAA
handle3-4	AGGAATAGTTATAATTCAACCGCAAAGGAACGGCATGATTGCTA
handle3-5	AGGAATAGTTATAAAATCAAGGTTAGAAAATACATACATAAATATT
handle3-6	AGGAATAGTTATAATAATTCAATTCTTAACTCCGGCTTAGATTATAATGGACTCA
handle3-7	AGGAATAGTTATAAAATCATAATTCAAATGGTTATAACTATCTG
handle3-8	AGGAATAGTTATAAGCCAAAGGTTATTATAATAACGGAATATTA
handle3-9	AGGAATAGTTATAAGCTTAATTGAGCCTGTTATCAACAAATATCCTAAAGCAAGCCGTC
handle3-10	AGGAATAGTTATAAAAGCCAAATAAGTCAGCTAATGCAGA
handle3-11	AGGAATAGTTATAACTGTTACAAAGAATGCTGATGCAAATCAATTATCTGCTTCTGA
handle3-12	AGGAATAGTTATAAAATACAAAAGTAATTCTGTATCGCAAGAGTATCATCCGACTT
90-strut	
90-1-1	TGATGCCTATTCTAACATTATGACCCGTAAATGTAAACGTTAATATTTGTT
90-1-2	AGGTTACCTGCTTATCGATGAACGGTAATCGTAAGTGTAGGTAAGATTCAAAG
90-1-3	TATTCGCATGGCCCTTTCGGGAGAACCTTATGTATAAGCAAATATTTAAAT
90-1-4	GATTTCCAGAACTAACTAGCATGTCAATCATATGTAAATGCAATGCCGTAGTAAT
90-1-5	GCTGACTTATTAAATTCAACGCAAGGATAAAATTAGAACCCCTCATATATT
90-1-6	ATCTCGATGTAAGTACCCGGTTGATAATCAGAAAGCCCCAAAAACAGGAAGAT
90-2-1	TTAATGCCGTATGCTTAGCGTTGCCATTTCAACCTATTATTGAAACATGA
90-2-2	TTGTATAGCCAACCTGGCTTGTGATGATAACAGGAGCCACCCCTCAGAGCCGCCACCA
90-2-3	GATTTCTACCGTATAATCAAATCACCGGAACCAATGCCCTGCCATTTCGGA
90-2-4	TTACCAATTGGTGTGTACTGGTAATAAGTTAAGAACCGCCACCTCAGAGCCA

90-2-5	TGTCTCGTAAGGTTGAGCCACCACCGAACCGCCTCCCTCAGAGCCGCCACCCCTCA
90-2-6	GTTATTCGACTAGCCGGGTCAGTGCCTGAGTAACAGTGCCGTATAAACAGTTA
90-3-1	AGTTCCCTGAGGTAAACCACCAAGCAGAAGATAAAAAGCGGAATTATCATCATATTC
90-3-2	GACTTGCTATAAAGTACAACAAATTGACAACACTCGCTTGCTGAACCTCAAATATCA
90-3-3	CTTAAGCTGTCTCTCAGAGGTGAGGCAGTCAGTATAACAAAGAAACCACCAAGG
90-3-4	AGATTGTCTCGTGTATTAAATCCTTGCCCCAACATGAAAAATCTAAAGCATCAC
90-3-5	TCTATGTAGCGTCATAACACCGCCTGCAACAGTGCACGCTGAGAGCCAGCAGCAA
90-3-6	CTAGGATTCCCGGGTTATTAATTAAAAGTTGAGTAACATTATCATTGCGG
	90-strut release
R-90-1-1	AACAAAATATTAACGTTACATATTACAGGGTCATAATGTTAAGAATAGGCATCA
R-90-1-2	CTTTGAATCTTACCTACACTACGATTACCGTTACGATAAGCAAGGTAAACCT
R-90-1-3	ATTTAAATATTGCTTATACATAAAGGCTCTCCCGCAAAGGGACCATGCGAATA
R-90-1-4	ATTACTCAGGCATTGCATTACATATGATTGACATGCTAGTTAGTTCTGGAAAATC
R-90-1-5	AAATATATGAGGGTTCTAAAATTTTATCCTTGCGTTGAAATTAAAGTCAGC
R-90-1-6	ATCTTCCTGTTTGGGCTTTCTGATTATCAACCGGGTACTTACATCGAGAT
R-90-2-1	TCATGTTTCAGAATAATAGGTGAAAAGATGGCAAACGCTAACGCATACGGCATTAA
R-90-2-2	TGGTGGCGGCTCTGAGGGTGGCGTTCTAAAACCTTATTACCAAGTACACACACCAATGGTAA
R-90-2-3	TCCGAAATAGGCAGGGGGCATTGGTCCGGTGATTTGATTACCGTAGAAATC
R-90-2-4	TGGCTCTGAGGGTGGCGTTCTTAAACCTTATTACCAAGTACACACACCAATGGTAA
R-90-2-5	TGAGGGTGGCGGCTCTGAGGGAGGCGGTCCGGTGGCTAACCTTACGAGACA
R-90-2-6	TAACTGTTATACGGCACTGTTACTCAAGGCACTGACCCGGCTAGTCGAATAAC
R-90-3-1	GAATATGATGATAATTCCGTTTATCTCTGCTGGTTACCTCAAGGAAC
R-90-3-2	TGATATTGAGGTTCAAGCAACGGAGTTGCAATTGTTACTTATAGCAAGTC
R-90-3-3	CCTCTGGTGGTTCTTGTATACTGACCGCCTCACCTCTGAGAGACAGCTTAAG
R-90-3-4	GTGATGCTTAGATTTTATGTTGGCAAAGGATTAAATAACACGAGACAATCT
R-90-3-5	TTGCTGCTGGCTCTCAGCGTGGCACTGTTGCAGGCGGTGTTATGACGCTACATAGA
R-90-3-6	CCGCAAATGATAATGTTACTCAAACTTAAAATTAATAACCGGGAAATCTAG
	60-strut
60-1-1	ATTAGTCTGCGCATAAACATTATGACCCGTAAATGTAACGTTAATATTGTT
60-1-2	TTAGCTGCACGTAATCGATGAACGGTAATCGTAAGTGTAGGTAAGATTCAAAG
60-1-3	ATTATGCGTCACGTCTTTCGGGAGAACCTTATAATGCAATGCCGTAGTAAT
60-1-4	ATGCTACTTGTGAAACTAGCATGTCAATCATATGTTAGCAAGCAAATATTAAAT
60-2-1	CTAATGTCTGACGTTAGCGTTGCCATCTTCAACCTATTCTGAAACATGA
60-2-2	CTGCTTGAACCGCGTGGCTTGATGATACAGGAGCCACCCCTCAGAGCCACCA
60-2-3	ACCTGAGTTCTGTAATCAAACACCGGAAACAGAACCGCCACCCCTCAGAGCCA
60-2-4	GTACTTGCTAAAGTGTACTGGTAATAAGTTTAAATGCCCTGCCATTTCGGA
60-3-1	TTTACTGCGAGTCCAACCACCAAGCAGAAGATAAAAAGCGGAATTATCATCATATT
60-3-2	TGCCAGTTATCTCTACAAACAAATTGACAACACTCGCTGCTGAACCTCAAATATCA
60-3-3	TCTACTGTAGCCCACAGAGGTGAGGCAGTCAGTATATGAAAAATCTAAAGCATCAC
60-3-4	CGTTCTTAAGTCGTTAAATCCTTGCCCCAACACAAAGAAACCACCAAGAAGG
	60-strut release
R-60-1-1	AACAAAATATTAACGTTACATATTACAGGGTCATAATGTTATGCGCAGACTAAT
R-60-1-2	CTTTGAATCTTACCTACACTACGATTACCGTTACGTTACGCTAA
R-60-1-3	ATTACTCAGGCATTGCATTATAAAGGCTCTCCGCAAAGACGTGACGCATAAT

R-60-1-4 ATTAAATTTGCTTACACATATGATTGACATGCTAGTTCGACAAGTAGCAT

R-60-2-1 TCATTTCAGAATAATAGTTGAAAAGATGGCAAACGCTAACGTCAGACATTAG

R-60-2-2 TGGTGGCGGCTCTGAGGGTGGCTCTGTATCATCAAAAGCCACGCCGTTCAAAGCAG

R-60-2-3 TGGCTCTGAGGGTGGCGGTCTGGTCCGGTGATTTGATTACAGGAAACTCAGGT

R-60-2-4 TCCGAAATAGGCAGGGGGCATTAAAACCTATTACAGTACACTTTAGCAAGTAC

R-60-3-1 GAATATGATGATAATTCCGCTTTTATCTCTGCTGGTGGTGGACTCGCAGTAAA

R-60-3-2 TGATATTGAGGTTCAGCAAGCAGTTGCGAATTGTTGTAGAGATAAACTGGCA

R-60-3-3 GTGATGCTTAGATTTCATATACTGACCGCCTCACCTCTGTGGCTACAGTAGA

R-60-3-4 CCTCTGGTGGTTCTTGTGTCGGGAAAGGATTAATAGCGACTTAAGAACG

30-strut

30-1-1 TGATATCGCATTAAACATTATGACCCTGTAATAGTAGGTAAGATTCAAAG

30-1-2 CGTAATCTGCTTATCGATGAACGGTAATGTAATGTAACGTTAATATTGTT

30-2-1 TGGCTTCAGTCCTAGCGTTGCCATTTTACACCACCTCAGAGCCGCCACCA

30-2-2 CGATTGCTAGCGTTGGCTTGATGATAACAGGAGACCTATTATTGAAACATGA

30-3-1 ATATCGTCGTACAACCACCGAGAAAGATAAAACTGCTGAACCTCAAATATCA

30-3-2 TTCATTGGACCTGGTACAAACAATTGACAACTCGAGCGGAATTATCATCATATT

30-strut release

R-30-1-1 CTTTGAAATCTTACACTATTACAGGGTCATAATGTTAATCGCAGATATCA

R-30-1-2 AACAAAATATTAACGTTTACATTACGATTACGTTATCGATAAAAGCAAGATTACG

R-30-2-1 TGGTGGCGGCTCTGAGGGTGGTAAAAGATGGCAAACGCTAAGGACTTGAAAGCCA

R-30-2-2 TCATTTCAGAATAATAGGCTCCTGTATCATCAAAAGCCAACGCTAGCAAATCG

R-30-3-1 TGATATTGAGGTTCAGCAAGTTTATCTCTGCTGGTGGTTGTAGACGACGATAT

R-30-3-2 GAATATGATGATAATTCCGCTCGAGTTGCGAATTGTTGTACCGGTCAAATGAA

PAINT handle

vertex CAAAATTAAATTACATTAACTTACATA

vertex CCTCAGAACGCCACCCTCATTATCTACATA

vertex AACAGTACCTTTACATCGTTATCTACATA

vertex TTAGCGTAACGATCTAAAGTTATCTACATA

vertex CCTCAGCAGCGAAAGACAGCTTATCTACATA

vertex GTAATGGGATAGGTACGTTTATCTACATA

vertex TGCCATCTGTAAGCAACTCGTTATCTACATA

vertex GGCAAAGCGCCATTGCCATTCTACATA

vertex TGGTTGAAATACCGACCCTTATCTACATA

End TTAACACCAGAACGAGTCTGCCCTGACGGAGATTATCTACATA

End TTAACATGTAATTTCTGAACATTATCTACATA

End TTCCCTGAGAGAGTTGCCCTTCACCGCCTGGTTATCTACATA

End TTGGGACATTCCAGACAATATTTATCTACATA

End TTCAAACATCGCGTAATAAAATTATCTACATA

End TTTTGCCCCGATAAAATCATACATTATCTACATA

End TTAGAAGGAAACCGAGGCCAACAAAGTTACCTTATCTACATA

End TTACCATACCTCAGTAGGGACATTATCTACATA

End TTTGACCCCCAGCGCCAACCTTGTTATCTACATA

End TTATTCAATGGTACCGAGTAGCTTATCTACATA

End TTGCTAAACAGGAGGCCAGAACAGAGCGGGATTATCTACATA

End TTCTGTAGCTAACATATTCATTATCTACATA
End TTATCATTACCGCGCCCATTTCATCGTAGGATTATCTACATA
End TTAAAAAGATTAAGAGGAAAGCGGATTGCATCTTATCTACATA
End TTGAGCTCGAATTCTCACTGCCTTATCTACATA

V. References

- S1. Jana, N. R.; Gearheart, L.; Murphy, C. J., Seed-Mediated Growth Approach for Shape-Controlled Synthesis of Spheroidal and Rod-Like Gold Nanoparticles Using a Surfactant Template. *Adv. Mater. (Weinheim, Ger.)* **2001**, *13*, 1389-1393.
- S2. Shi, D. W.; Song, C.; Jiang, Q.; Wang, Z. G.; Ding, B. Q., A Facile and Efficient Method to Modify Gold Nanorods with Thiolated DNA at a Low pH Value. *Chem. Commun. (Cambridge, U. K.)* **2013**, *49*, 2533-2535.
- S3. Liu, N.; Langguth, L.; Weiss, T.; Kastel, J.; Fleischhauer, M.; Pfau, T.; Giessen, H., Plasmonic Analogue of Electromagnetically Induced Transparency at the Drude Damping Limit. *Nat. Mater.* **2009**, *8*, 758-762.
- S4. Zhang, S.; Genov, D. A.; Wang, Y.; Liu, M.; Zhang, X., Plasmon-Induced Transparency in Metamaterials. *Phys. Rev. Lett.* **2008**, *101*, 047401.
- S5. Yun, B. F.; Hu, G. H.; Cong, J. W.; Cui, Y. P., Fano Resonances Induced by Strong Interactions between Dipole and Multipole Plasmons in T-Shaped Nanorod Dimer. *Plasmonics* **2014**, *9*, 691-698.